

## HIGH ISOLATION DBR DIPLEXER USING IN-LINE SCMRC

C. Chen\*, H. Wu, and W. Wu

Ministerial Key Laboratory of JGMT, Nanjing University of Science and Technology, Nanjing 210094, China

**Abstract**—A new microstrip diplexer with very high output isolation and low insertion losses is presented in this letter. With the adoption of the spiral compact microstrip resonant cell (SCMRC) form into the dual behavior resonator (DBR) microstrip filter design, a bandpass filter with high rejection in the upper stopband can be achieved. Therefore, very high output isolation for the diplexer can be realized. Furthermore, the proposed diplexer also has a property of low insertion loss in the passband. To validate the design theory, one demonstrator diplexer has been designed and fabricated; the results indicate that the proposed diplexer has good performance of simple structure, better than 65 dB output isolation in the stopband, and less than 1.2 dB insertion losses in the passband.

### 1. INTRODUCTION

The diplexer is an essential component in modern wireless communication systems. The transmitter and receiver operate in different frequency bands and are duplexed to the antenna by the transceiver diplexer. So the diplexer often consists of a Tx-filter, an Rx-filter and a  $T$ -junction. To satisfy stringent system requirements, diplexers with high isolation and low insertion losses are necessary. From the cost point of view, planar structures are primarily preferable for diplexer applications.

A variety of high isolation microstrip dippers have been reported in the literature. Typically, to achieve very high diplexer output isolation performance, filter topologies that can result in transmission zeros are preferred in the microstrip diplexer design [1–7]. In [1],

---

*Received 12 May 2011, Accepted 2 June 2011, Scheduled 17 June 2011*  
\* Corresponding author: Chun Hong Chen (chunhong\_chen@qq.com).

an S-band hairpin diplexer is presented, and the isolations are more than 40 dB. Hairpin topology is considered to be appropriate approach for placing the transmission zeros, but the desired rejection is still not achieved. Stepped impedance resonator filter has found wide application with the advantage of adjustable parasitic passband. The diplexer composed of two dual-mode ring bandpass filters using the stepped-impedance resonator is designed and fabricated in [2], a high isolation greater than 40 dB between two channels is obtained. And in [3], a diplexer using the modified stepped-impedance resonators is presented, so wide and deep stopbands for the BPFs are obtained. A stepped impedance coupled line based hairpin diplexer is presented in [4], the spurious response level is below 50 dB at the upper stopband, and the isolations are more than 40 dB. In [5, 6], two Chebyshev-type cross-coupled planar microwave filters with a pair of attenuation poles near cut-off frequencies are utilized in the dplexers, and the simulated isolations are better than 40 dB. The diplexer with hybrid resonators is proposed in [7], the resonator is a combination of a shunt resonant circuit and series resonant circuit, and the output isolation is measured better than 55 dB. However, in the aforementioned works, due to the restriction of the fabrication process, manufacturing tolerances influence the passband performance and cause a shift of the center frequency. The complex circuit structures and requirements of high fabrication tolerance limit their application in the wireless communication systems. Furthermore, more than 60 dB diplexer isolations are demanded in modern system such as remote communication systems. Therefore, further improvement should be carried out on both simple diplexer topology and higher transceiver isolation.

On account of the characteristics of low insertion loss, flatness and easiness to design, much effort has been made in the past years to develop the dplexers using the DBR topology [8–10]. In [8–10], the oversized DBR is used for getting a high rejection level, and in [10], a notch in the transmission line also is introduced to improve rejection at the receiving/transmitting bands. Nevertheless, the transceiver isolation of above-mentioned DBR diplexer is not high enough.

This article presents the design and development of a microstrip diplexer using the DBR approach. To achieve the desired specifications, two filters at the Rx and Tx frequency bands are optimized. The SCMRC is introduced into the Rx-filter to improve the upper stopband rejection, so very high transceiver isolation can be achieved. At the same time, by using the SCMRCs instead of two admittance inverters, the circuit size is reduced. Further, a suitable T-junction has been designed to integrate the Rx and Tx

filters for the diplexer arrangement. Details of the diplexer design and characteristics are described, and experimental results are presented. Measured results indicate that the designed diplexer has better than 65 dB transceiver isolations, together with less than 1.3 dB insertion losses, which agree well with simulation results.

## 2. DESIGN CONCEPT

### 2.1. DBR Filter

DBR is a basic resonator that presents a dual frequency behavior in the pass band and stop band regions, which are studied in detail in [11, 12]. DBRs are based on the parallel association of two different bandstop structures, which implies a constructive recombination. According to the number of available parameters and to the initial behavior of each bandstop structure, DBR allows an independent control of the following:

- one pole in the operating bandwidth;
- one transmission zero in the lower attenuated band;
- one transmission zero in the upper attenuated band.

There are several topologies based on the DBR concept. The DBR based on two open-circuited stubs is the easiest to implement. Figure 1 illustrates the DBR filter based upon different-length open-circuited stubs. These DBRs can now be modeled by their equivalent slope parameter  $b$ . For an  $n$ th-order DBR filter, the  $j$ th resonator can

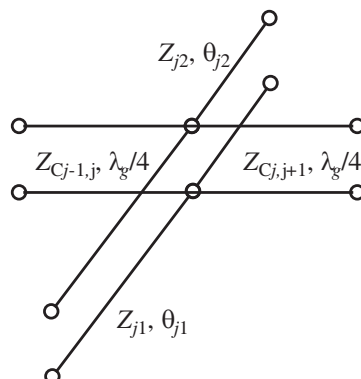


**Figure 1.** DBR filter based upon different-length open-circuited stubs.

be defined as follows [11]:

$$\theta_{j1} = \frac{\pi}{2k_{j1}} \quad (1)$$

$$\theta_{j2} = \frac{\pi}{2k_{j2}} \quad (2)$$

$$Z_{j1} = -\frac{Z_{j2} \tan \theta_{j1}}{\tan \theta_{j2}} \quad (3)$$

$$Z_{j2} = Z_0 \frac{\pi}{b_j} \left[ \frac{1 + \tan^2 \theta_{j2}}{4k_{j2}} - \frac{(1 + \tan^2 \theta_{j1}) \tan \theta_{j2}}{4k_{j1} \tan \theta_{j1}} \right] \quad (4)$$

where the  $k_{jk}$  is the ratio of the frequency of transmission zero to the central frequency.

As the resonators are characterized by a proper  $b_j$  coefficient, the designer only needs to calculate the characteristic impedances  $Z_{Cj,j-1}$  of the quarter-wavelength admittance inverters defined as follows [11]:

$$Z_{C01} = Z_0 \sqrt{\frac{g_a b_1 w}{\omega'_1 g_0 g_1}} \quad (5)$$

$$Z_{Cj,j+1} = Z_0 \sqrt{\left( \frac{w}{\omega'_1} \sqrt{\frac{b_j b_{j+1}}{g_j g_{j+1}}} \right)} \quad (6)$$

$$Z_{Cn,n+1} = Z_0 \sqrt{\frac{g_b b_n w}{\omega'_1 g_n g_{n+1}}} \quad (7)$$

where the  $g_j$ 's are the Chebyshev coefficients of the equivalent low-pass filter prototype and define the bandwidth ripple, the parameter  $\omega'_1$  is the cutoff frequency of the low-pass prototype,  $g_a$  and  $g_b$  are the terminating conductances of the circuit, and  $w$  is defined as the fractional bandwidth.

By using the synthesis described by the above equations, the Tx-filter and the Rx-filter used for the C-band satellite communication system are designed. The passband of the Rx-filter is chosen from 3.7 to 4.2 GHz, and which of the Tx-filter is 5.9 ~ 6.4 GHz. In order to obtain high isolation of the diplexer, considerable stopband suppression for Rx-filter is particularly required in the 5.9 ~ 6.4 GHz band. On the other hand, high stopband suppression within the band of 3.7 ~ 4.2 GHz is required for Tx-filter.

The use of (1)–(7) in association with the input parameters reported in Table 1 led to the output parameters displayed in Table 2. Figure 2 illustrates the associated electrical response of the filters. As shown in Figure 2(a), the Tx-filter presents a high rejection level of

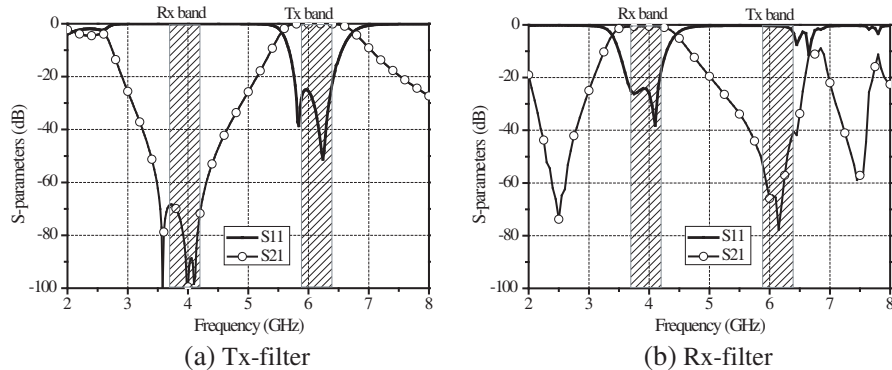


**Figure 2.** Simulation performance of the DBR filters.

**Table 1.** Input parameters of the third-order DBR filters (0.01 dB ripple).

	Tx-filter	Rx-filter
Filter	$F_0 = 6.15 \text{ GHz}$ , $w = 12\%$	$F_0 = 3.95 \text{ GHz}$ , $w = 17\%$
DBR1	$k_{11} = 0.57$ , $k_{12} = 1.6$	$k_{11} = 0.65$ , $k_{12} = 1.49$
DBR2	$k_{21} = 0.64$ , $k_{22} = 1.6$	$k_{21} = 0.65$ , $k_{22} = 1.56$
DBR3	$k_{31} = 0.68$ , $k_{32} = 1.6$	$k_{31} = 0.65$ , $k_{32} = 1.62$

**Table 2.** Output parameters of the third-order DBR filters.

	Tx-filter	Rx-filter
DBR1	$Z_{11} = 25.46$ , $\theta_{11} = 157.89$ $Z_{12} = 93.81$ , $\theta_{12} = 56.25$	$Z_{11} = 32.44$ , $\theta_{11} = 138.46$ $Z_{12} = 64.47$ , $\theta_{12} = 60.40$
DBR2	$Z_{21} = 36.57$ , $\theta_{21} = 140.63$ $Z_{22} = 66.69$ , $\theta_{22} = 56.25$	$Z_{21} = 31.44$ , $\theta_{21} = 138.46$ $Z_{22} = 56.12$ , $\theta_{22} = 57.69$
DBR3	$Z_{31} = 46.38$ , $\theta_{11} = 132.35$ $Z_{32} = 63.28$ , $\theta_{12} = 56.25$	$Z_{31} = 30.77$ , $\theta_{11} = 138.46$ $Z_{32} = 50.65$ , $\theta_{12} = 55.56$
Inverter	$Z_{C01} = Z_{C34} = 57.24$ $\theta_{C01} = \theta_{C34} = 90$ $Z_{C12} = Z_{C23} = 81.38$ $\theta_{C01} = \theta_{C34} = 90$	$Z_{C01} = Z_{C34} = 43.02$ $\theta_{C01} = \theta_{C34} = 90$ $Z_{C12} = Z_{C23} = 45.96$ $\theta_{C01} = \theta_{C34} = 90$

about 66 dB in the Rx-band, insertion losses of 0.4 dB and flatness of 0.2 dB in the bandwidth. From Figure 2(b), we can see that the Rx-filter also has the insertion losses of 0.4 dB and flatness of 0.2 dB in the bandwidth, nevertheless the rejection level in the Tx-band is not enough because of the influence of the spurious response at 6.7 GHz nearby.

This topology allows placing independent transmission zeros at prescribed frequencies. Indeed, when considering a given rejection level, these transmission zeros result in a reduction of the filter order and, therefore, reduce the losses of the whole structure. Compared to the traditional coupled line topology, significant improvements should be noted. In particular, the DBR and associated synthesis allow control of the bandwidth together with two attenuated bands. Moreover, no additional tunability difficulties are encountered thanks to the independence of the two bandstop structures. Nevertheless, the main problem of this kind of resonator is the spurious response. Further studies should focus on the integration of low-pass structures.

## 2.2. DBR Filter with SCMRCs

The compact microstrip resonant cell (CMRC), as first proposed in [13], is a quasi-lumped circuit element. At the resonant frequency, the cell exhibits a bandstop characteristic, making it a low-pass filter. Its compactness makes it suitable for various passive and active circuit applications.

Figure 3 shows the structure of the SCMRC proposed in [14]. As can be seen from Figure 3, this SCMRC consists of four folded lines, which make the structure a slow-wave transmission line. Also, the nonuniform increments of inductance and capacitance in the structure lead to multipoint resonance, which results in a wide bandstop effect. The SCMRC should be properly designed to obtain the needed wide stopband, while maintaining a low insertion loss over the passband region. This structure features a very simple yet compact one-dimensional (1-D) design that offers broad stopband and excellent

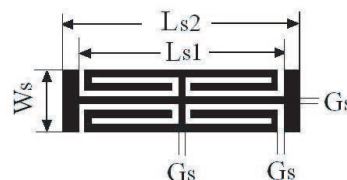


**Figure 3.** Layout of SCMRC.

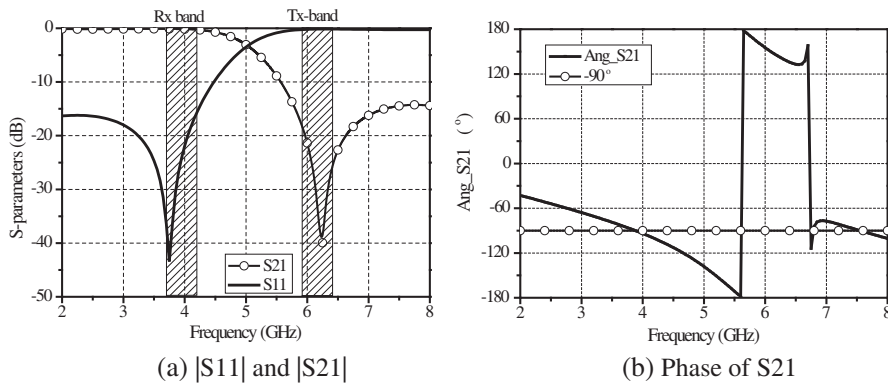


**Figure 4.** Simulated  $S$ -parameters of SCMRC.

**Table 3.** Parameters of the SCMRC.

Substrate		SCMRC			
$\varepsilon_r$	$h$	$W_s$	$L_{s1}$	$L_{s2}$	$G_s$
2.2	0.254 mm	2.7 mm	4.6 mm	5 mm	0.1 mm

slow-wave characteristics.

It is appropriate to introduce SCMRC into Rx-filter to improve the rejection in the upper stopband. To avoid size increasing, SCMRCs are used to replace the admittance inverters of Rx-filter. For matching purpose, the width of the cell ( $W_s$ ) should be carefully adjusted to attain the impedance equal to the characteristic impedance of the quarter wavelength admittance inverter. A short microstrip line can be added near the SCMRC to insure that the transmission phase is  $90^\circ$  at the center frequency of Rx-filter.

A C-band SCMRC low pass filter is studied, and the dimension parameters are listed in Table 3. Figure 4 shows the simulated  $S$ -parameters. From Figure 4, it can be seen that the relative stopband better than  $-10$  dB covers the frequency range of  $5.5 \sim 8$  GHz.

As shown in Figure 5, the aforementioned SCMRC is introduced into Rx-filter. Figure 6 shows the simulated results of Rx-filter without SCMRC and with SCMRC, respectively. As observed, the upper spurious resonances are suppressed, and the suppression of the upper stopband is improved to better than  $60$  dB. Meanwhile, the performance in passband is unchanged.

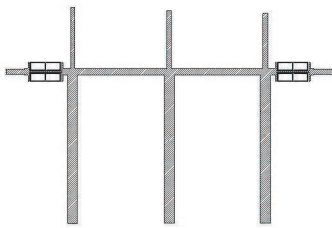


**Figure 5.** Layout of Rx-filter with SCMRC.

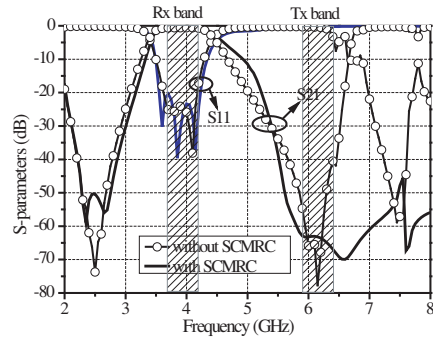


**Figure 6.** Simulated results of Rx-filter without SCMRC and with SCMRC.

### 2.3. Diplexer

The  $T$ -junction is an essential part of the diplexer to join both the Tx and Rx filters without influence between each other. Lastly, to obtain satisfactory impedance matching, the input impedance at the  $T$ -junction needs to satisfy the following conditions [7]:

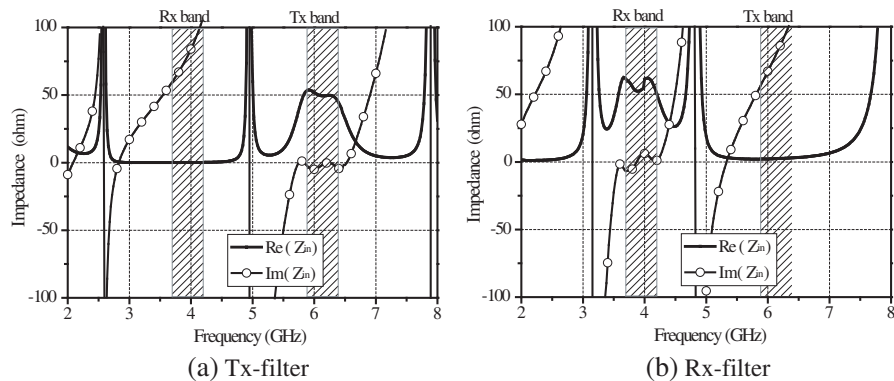
$$Z_{in\_Tx} = \begin{cases} \infty, & \text{in Rx band} \\ 50\Omega, & \text{in Tx band} \end{cases} \quad (8)$$

$$Z_{in\_Rx} = \begin{cases} 50\Omega, & \text{in Rx band} \\ \infty, & \text{in Tx band} \end{cases} \quad (9)$$

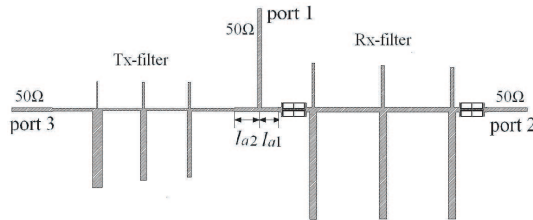
where  $Z_{in\_Tx}$  and  $Z_{in\_Rx}$  are the input impedances of the diplexer at the  $T$ -junction looking into the upper and lower path, respectively

Figure 7 illustrates the input impedances of Tx and Rx filters. From Figure 7, we know that both input resistances of the Tx-filter in Rx band and the Rx-filter in Tx band are very low, so the  $50\Omega$  microstrip lines with the appropriate lengths are added at the Tx/Rx filter port, to transform the low resistances to open circuits at the  $T$ -junction. And the lengths of the  $50\Omega$  lines can be calculated according to the reactance of the Tx/Rx filter. The Tx and Rx filters are joined together using the  $T$ -junction and further optimization is carried out to get the desired response.

The geometry of the proposed diplexer is depicted in Figure 8. As shown in Figure 8, the lengths of the  $50\Omega$  lines are  $l_{a1} = 3.8$  mm and  $l_{a2} = 5$  mm, respectively, so there is influence on neither return loss, nor insertion loss.



**Figure 7.** Input impedances of Tx and Rx filters.



**Figure 8.** Layout of the proposed diplexer.

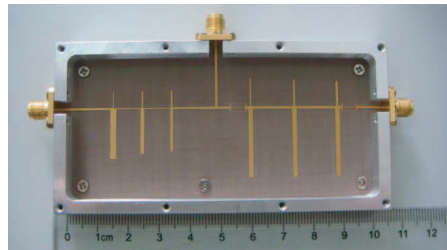


**Figure 9.** The photograph of the fabricated diplexer.

### 3. SIMULATION AND MEASUREMENT

The diplexer was fabricated on a 0.254 mm thick Rogers 5880 substrate with a dielectric constant  $\epsilon_r = 2.2$ , and the final photograph of the fabricated diplexer with size  $95 \times 43 \text{ mm}^2$  is shown in Figure 9. The simulated (carried out by Ansoft HFSS) and measured (carried out by Agilent 8722ES vector network analyzer) results are shown in

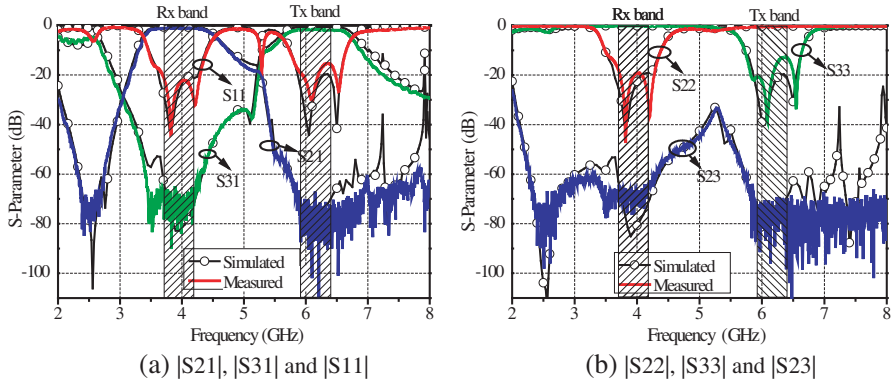


**Figure 10.** Simulated and measured  $S$ -parameters of the proposed diplexer.

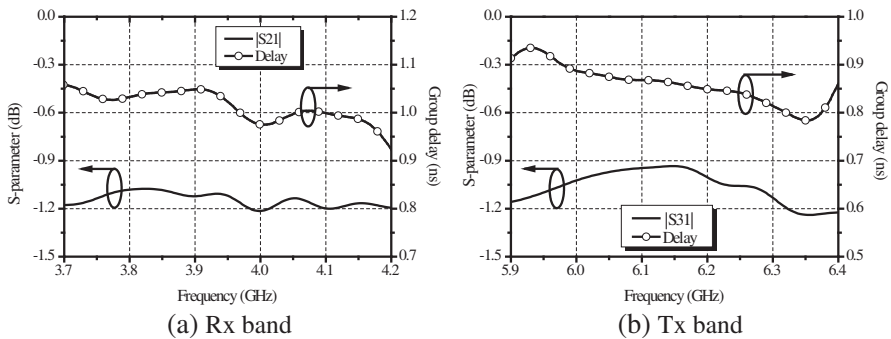


**Figure 11.** Measured insertion loss and group delay of the proposed diplexer in Rx/Tx band.

Figure 10. Obviously, there are good agreements between simulation and measurement. The return losses are better than 14 dB, and both measured stopband suppressions are better than 63 dB. The output isolation was measured better than 65 dB. Figure 11 illustrates the insertion loss and group delay variation in the pass-bands. The insertion loss is  $1.15 \pm 0.05$  dB in Rx band and  $1.05 \pm 0.15$  dB in Tx band. Furthermore, the group delay is  $0.99 \pm 0.07$  ns in Rx band and  $0.86 \pm 0.08$  ns in Tx band, respectively. So, we can say that the filter phases are approximately linear in the passbands. The increase of insertion loss may be caused by junction discontinuities in printed circuit board with SMA connectors.

#### 4. CONCLUSION

A microstrip DBR diplexer with the SCMRC form adopted has been studied. Using this structure, a C-band diplexer has been designed, fabricated and measured. Results indicate that the proposed diplexer demonstrates many attractive features with simple structure, better than 65 dB output isolation in the stopband, and less than 1.2 dB insertion losses in both passbands. Actually, this proposed diplexer is very suitable for the microstrip circuit implementation in dual-band wireless systems, such as satellite communication systems and cellular base stations.

#### REFERENCES

1. Zhang, A., D. He, and Q. Yin, "Design of diplexer based on microstrip tapped-hairpin filter with frequency in S-band," *Modern Electronics Technique*, Vol. 19, 11–13, 2007.
2. Huang, C. Y., M. H. Weng, C. S. Ye, and Y. X. Xu, "A high band isolation and wide stopband diplexer using dual-mode stepped-impedance resonators," *Progress In Electromagnetics Research*, Vol. 100, 299–308, 2010.
3. Yang, R. Y., C. M. Hsiung, C. Y. Hung, and C. C. Lin, "Design of a high band isolation diplexer for GPS and WLAN system using modified stepped-impedance resonators," *Progress In Electromagnetics Research*, Vol. 107, 101–114, 2010.
4. Sarayut, S., P. Sumongkol, P. Ravee, B. Sawat, K. Sompol, and C. Mitchal, "High isolation and compact size microstrip hairpin diplexer," *Microw. Wirel. Comp. Lett.*, Vol. 15, No. 2, 101–103, 2005.
5. Chen, Y. C., H. F. Cheng, C. M. Lei, and I. N. Lin, "Chebyshev-type dippers designed using coupling matrix method," *Mater. Chem. Phys.*, Vol. 79, No. 2–3, 116–118, 2003.
6. Han, S., X. L. Wang, Y. Fan, Z. Yang, and Z. He, "The generalized Chebyshev substrate integrated waveguide diplexer," *Progress In Electromagnetics Research*, Vol. 73, 29–38, 2007.
7. Yang, T., P. L. Chi, and T. Itoh, "High isolation and compact diplexer using the hybrid resonators," *Microwave Wirel. Comp. Lett.*, Vol. 20, No. 10, 551–553, 2010.
8. Manchec, A., R. Bairavasubramanian, C. Quendo, S. Pinel, E. Rius, C. Person, J. F. Favenne, J. Papapolymerou, and J. Laskar, "High rejection planar diplexer on liquid crystal

- polymer substrates using oversizing techniques," *Microwave Conference, European*, Vol. 1, 2005.
- 9. Manchec, A., E. Rius, C. Quendo, C. Person, J. F. Favennec, P. Moroni, J. C. Cayrou, and J. L. Cazaux, "Ku-band microstrip diplexer based on dual behavior resonator filter," *Microwave Symposium Digest, IEEE MTT-S International*, 525–528, 2005.
  - 10. Singh, K., K. Ngachenchaiah, D. Bhatnagar, and S. Pal, "Notch implemented dual behavior resonator filter and diplexer at Ku-band," *Microwave Journal*, Euro-Global Edition, Vol. 53, 206–216, 2010.
  - 11. Quendo, C., E. Rius, and C. Person, "Narrow bandpass filters using dual-behavior resonators," *IEEE Trans. Microw. Theory Tech.*, Vol. 51, No. 3, 734–743, 2003.
  - 12. Quendo, C., E. Rius, and C. Person, "Narrow bandpass filters using dual-behavior resonators based on stepped-impedance stubs and different-length stubs," *IEEE Trans. Microw. Theory Tech.*, Vol. 52, No. 3, 1034–1044, 2004.
  - 13. Xue, Q., K. M. Shum, and C. H. Chan, "Novel 1-D microstrip PBG cells," *IEEE Microwave Guided Wave Lett.*, Vol. 10, 403–405, 2000.
  - 14. Yum, T. Y., Q. Xue, and C. H. Chan, "Novel subharmonically pumped mixer incorporating dual-band stub and in-line SCMRC," *IEEE Trans. Microw. Theory Tech.*, Vol. 51, 2538–2547, 2003.